Understanding ^{6}He induced reactions at energies around the Coulomb barrier

A.M. Moro[*], L. Acosta[†], J.M. Arias[*], M. J. G. Borge[**], D. Escrig[**], J. Gómez-Camacho[*,‡], I. Martel[†], M. Rodríguez-Gallardo[**,*], A. M. Sánchez-Benítez[†] and O. Tengblad[**]

[*]*Departamento de Física Atómica, Molecular y Nuclear, Facultad de Física, Universidad de Sevilla, Apartado 1065, E-41080 Sevilla, Spain*
[†]*Departamento de Física Aplicada, Universidad de Huelva, E-21071 Huelva, Spain*
[**]*Instituto de Estructura de la Materia, CSIC, Serrano 113bis, E-28006 Madrid, Spain*
[‡]*Centro Nacional de Aceleradores, Av. Thomas A. Edison, E-41092 Sevilla, Spain*

Abstract. Recent developments aimed to understand the observed features arising in the scattering of the Borromean nucleus ^{6}He on heavy targets are discussed and compared with recent data for ^{6}He+^{208}Pb measured at the RIB facility at Louvain-la-Neuve at energies around the Coulomb barrier. The analysis of the elastic scattering data in terms of the optical model, reveals the presence of a long range absorption mechanism, that manifests in the form of a large value of the imaginary diffuseness parameter. The elastic data have been also compared with three–body CDCC calculations, based on a di-neutron model of ^{6}He, and four–body CDCC calculations, based on a more realistic three-body model of this nucleus. Finally, the angular and energy distribution of α particles emitted at backward angles are discussed and compared with different theoretical approaches. We find that these α particles are produced mainly by a two-neutron transfer mechanism to very excited states in the residual nucleus.

Keywords: Nuclear reactions, exotic beams, halo nuclei.
PACS: 25.45.De,24.10.Ht,24.10.Eq

INTRODUCTION

Nuclear reactions induced by radioactive beams constitute a major source of information on the properties of exotic nuclei. In the light region of the nuclear chart, the ^{6}He system is one of the most studied exotic nuclei, both from the experimental and theoretical sides. This nucleus exhibits many remarkable features: it consists on a tightly bound core (the α particle) and two loosely bound neutrons ($S_{2n} = 0.97$ MeV), β unstable ($\tau_{1/2} = 807$ ms) and constitutes a key example of Borromean system (a three-body system with no binary bound sub-systems), since both the neutron-neutron and α-neutron interactions are well known.

Reactions induced by ^{6}He on medium-mass and heavy targets at energies around the Coulomb barrier exhibit some common features: i) the elastic scattering does not follow the characteristic Fresnel pattern that happens in presence of strong absorption, and ii) a large yield of α particles. The behaviour (i) is known to be mainly related to the strong coupling to the continuum states due to the dipole Coulomb interaction. In order to understand this effect, the reaction ^{6}He+^{208}Pb was recently measured at the CYCLONE RNB facility at the Centre de Recherche du Cyclotron (CRC) of the

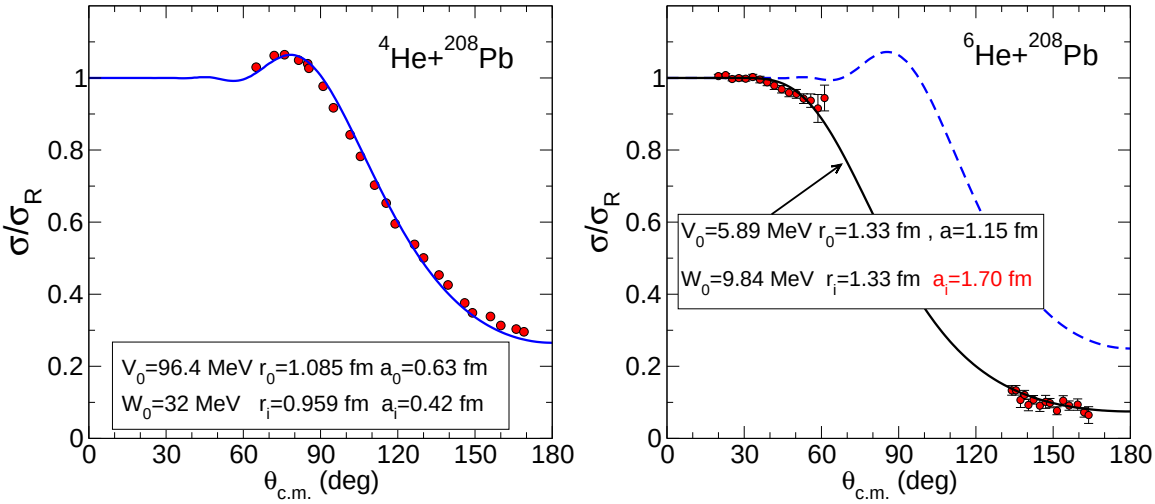

FIGURE 1. Differential elastic scattering cross section, relative to Rutherford, for ^{4}He+^{208}Pb and ^{6}He+^{208}Pb scattering at $E_{\rm lab} = 22$ MeV. The solid lines are optical model fits, with the parameters indicated in the boxes. The dashed line, is an optical model calculation for ^{6}He+^{208}Pb using the parameters for ^{4}He+^{208}Pb. Reduced radii indicated in the labels are to be multiplied by $A_1^{1/3} + A_2^{1/3}$ to be converted to physical radii.

Université Catholique de Louvain (UCL), Louvain-la-Neuve, Belgium. The experiments were performed at $E_{\rm lab}$=14, 16, 18, 22 MeV [1] and 27 MeV [1, 2], which correspond to energies below, around and above the Coulomb barrier. Along with the elastic data, the experiment recorded large amount of α particles, a feature that had been also observed in other ^{6}He induced reactions [3, 4].

In this work, we present some of the studies carried out by our group in order to understand the observed features of these data, along with previous existing data for ^{6}He scattering on several targets.

ANALYSIS OF THE ELASTIC SCATTERING

Optical model analysis

In Fig. 1 we compare the differential elastic cross section for ^{6}He+^{208}Pb at $E_{\rm lab} = 22$ MeV, from the present experiment, with previous data for ^{4}He+^{208}Pb corresponding to the same laboratory energy, taken from [5]. The ^{4}He data (left panel) displays the typical Fresnel pattern with an enhancement of the cross section around the rainbow angle, and a smooth decrease of the cross section beyond this angle. By contrast, in the ^{6}He case the interference maximum is completely suppressed, and the data displays a monotonous decrease with respect to the scattering angle.

In order to get a first insight on this behaviour, optical model calculations have been performed for the elastic angular distributions. The solid line in the left panel corresponds to an optical model (OM) calculation with the parameters indicated in the figure. If this potential is used for the ^{6}He+^{208}Pb reaction, one obtains the dashed line

in the right panel, which is in clear disagreement with the data due to the absence of the rainbow peak in the data.

Detailed calculations [1, 2, 6] clearly indicate that in order to reproduce the data, one requires an optical potential with a very large value of the real and imaginary diffuseness. One of such possible potentials is given by the solid line in this figure. In this case a diffuseness parameter as large as 1.15 fm and 1.70 fm for the real and imaginary parts, respectively, was required. This is a clear indication of the presence of long range absorption mechanism that is present in ^{6}He+^{208}Pb in contrast to the ^{4}He+^{208}Pb case. Given the loosely bound character of the halo neutrons, the main candidate for this mechanism is the strong polarizability of the projectile in the strong Coulomb and nuclear fields of the target.

Three-body CDCC calculations

The effect of the ^{6}He polarizability can be related to the couplings to the breakup states in the ^{6}He system. A convenient reaction model that takes into account explicitly these couplings is the Continuum-Discretized Coupled-Channels (CDCC) method. First applications of this method to the ^{6}He case have assumed a simple di-neutron model, in which the ^{6}He nucleus is treated as a two-body system, α+2n [4, 7]. In these works, the α-2n interaction is parametrized with some simple form (typically a Woods-Saxon shape) whose depth is adjusted in order to reproduce the two-neutron separation energy, $\varepsilon_b = -0.97$ MeV. However, this procedure produces a ground state wavefunction that extends too much in configuration space and, consequently, couplings to the continuum are largely overestimated. A possible interpretation for this result is that this extreme cluster model ignores the relative (positive) energy of the neutron pair. A possible improvement of this model, proposed in [8], is to define an effective α-2n separation energy, that is adjusted to reproduce the rms predicted within a three-body model. This procedure leads to an effective binding energy around $\varepsilon_b = -1.5$ MeV. We illustrate here the application of this improved di-neutron model to ^{6}He+^{208}Pb scattering. In these calculations, the α+2n relative wavefunction for the ^{6}He ground state is assumed to correspond to a pure $2S$ configuration, that is in fact the dominant configuration according to the predictions of three-body models. The α+2n interaction was parametrized in terms of a Woods-Saxon potential with radius $R = 1.9$ fm and diffuseness $a = 0.39$ fm which, with the present potential geometry, corresponds to a depth of $V_0 = 87.55$ MeV. We considered ℓ=0, 1 and 2 partial waves for the ^{6}He continuum. To generate the continuum states, we use the same potential geometry as for the ground state. For $\ell = 0, 1$ continuum states, we use the same depth found for the ground state. For $\ell = 2$, we take depth $V_0 = 92.2$ MeV in order to get the 2^{+} resonance at the correct excitation energy with respect to the ground state. Further details of this model can be found in [8].

The $2n$-Pb and α-Pb interactions, which are required to generated the ^{6}He+^{208}Pb coupling potentials, are taken from Refs. [9] and [5], respectively. For each ℓ, the continuum was truncated at 8 MeV and divided into 8 bins, equally spaced in the linear momentum. The result of this calculation is shown in Fig. 2 for $E_{\rm lab} = 22$ and 27 MeV. The full CDCC calculation, represented by the dashed line, explains very well

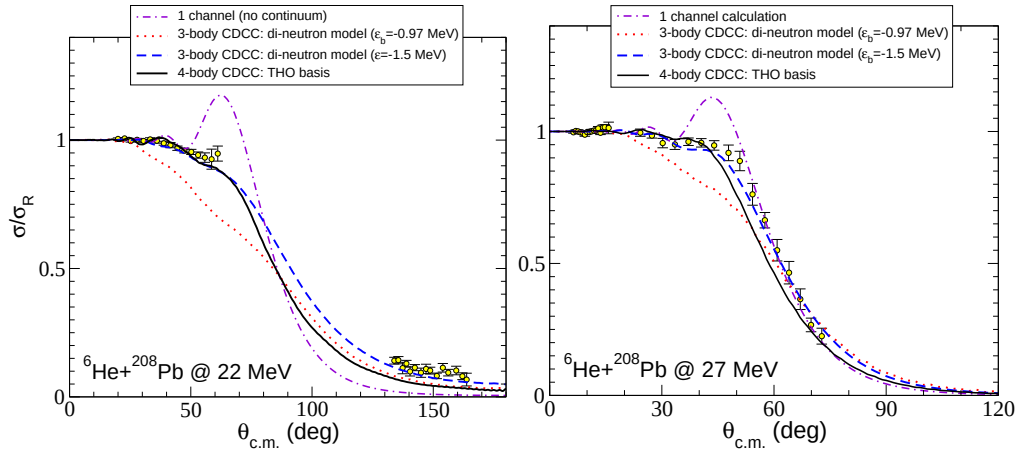

FIGURE 2. Elastic angular distribution for ^{6}He+^{208}Pb at 22 and 27 MeV, compared with CDCC calculations using the di-neutron model (dashed line) and three-body model of ^{6}He (solid line). The dot-dashed line is the one-channel calculation, in which couplings to the continuum are omitted.

the behaviour of the data. The dotted-dashed line in this figure is the CDCC calculation ignoring coupling to the continuum. The dotted line is the full calculation obtained in the di-neutron model using the two-neutron separation energy to generate the α-2n relative wavefunction, i.e., $\varepsilon_b = -S_{2n} = -0.97$ MeV. This calculation clearly overestimates the effect of the coupling to the continuum.

It has been also shown [10] that dipole Coulomb couplings are mainly responsible for the reduction of the cross section at the rainbow angles. Moreover, the equivalent polarization potential in this case consists of a relatively strong imaginary part of long range and a relatively weak, repulsive, long range real part, in agreement with the results found in the phenomenological OM analysis.

Four-body CDCC calculations

Despite the success of the simple di-neutron model, a full understanding of the reactions induced by a Borromean nucleus, such as ^{6}He, clearly requires a three-body description of the projectile. This demands a generalization of the CDCC method, which was originally formulated for two-body projectiles. This has been recently done by the Kyushu group [11, 12], as well as by our group [13], using in both cases a continuum representation in terms of pseudo-states. These pseudo-states are generated as the eigenstates of the internal (three-body) Hamiltonian of the projectile (^{6}He) in a family of square-integrable states. The Kyushu group uses a complex Gaussian basis, and expands the three-body function of the ^{6}He in Jacobi coordinates. In our approach, the three-body wavefunction is expanded in hyper-spherical coordinates using a Transformed Harmonic Oscillator (THO) basis [14], that we had previously applied to CDCC calculations with two-body projectiles [15].

In Fig. 2 we plot the results obtained with the four-body CDCC calculations based on the THO representation for ^{208}Pb at 22 and 27 MeV (solid lines). These calculations

describe very well the trend of the data in both cases, in particular, the suppression of the rainbow peak. Further details of these calculations can be found in [13].

An alternative to the pseudo-state procedure presented in this work would be the binning procedure, in which a representation of the continuum is generated by dividing the continuum into a set of energy (or momentum) intervals (*bins*) up to a maximum excitation energy. For each bin, a representative and normalizable wavefunction is constructed by making an appropriate superposition of positive energy states within the bin interval. In the ^{6}He case, this method requires the calculation of three-body scattering states. This work is still under progress and the results will be published elsewhere [16].

ANALYSIS OF THE TRANSFER/BREAKUP CROSS SECTION

A common feature of ^{6}He induced reactions is the large yield for α particles. For example, at 22 MeV the number of α particles detected at backward angles exceeds by a factor of 10 the number of ^{6}He at the same angles. This is consequence of the fact that the halo neutrons are loosely bound to the α core and hence they are easily removed due to the tidal forces exerted by the target. In the ^{6}He+^{208}Pb data discussed in this work, as well as in some other previous ^{6}He data, the neutrons were not measured, and hence there could be several mechanisms that may give rise to the production of the observed α particles. To shed light on this question, we have compared the data with theoretical calculations, assuming three different mechanisms. These models are schematically illustrated in Fig. 3 and correspond physically to the following situations:

(a) Direct breakup (DBU): The ^{6}He nucleus breaks up in the field of the target populating a continuum state with low excitation energy. In this case, we would expect that the α particle (and the neutrons) will have a similar velocity to the elastically scattered ^{6}He, and hence its energy would have a broad distribution around 4/6 of the energy of ^{6}He (Fig. 3a).

(b) Transfer to the continuum (TC): The ^{6}He nucleus gets close to the target, and the valence neutrons are transferred with low kinetic energy with respect to the ^{208}Pb nucleus, while the remaining α particle escapes. In this situation, the α particles will have an energy distribution centered around the energy of the elastically scattered ^{6}He (Fig. 3b).

(c) Neutron transfer (NT): This would correspond to an intermediate situation, in which one of the halo neutrons is transferred to the target, leaving the ^{5}He in a broad resonance, that will rapidly decay producing ^{4}He. In this case, the kinetic energy of the ^{5}He resonance, although Q-value dependent, would be similar to the elastically scattered ^{6}He (for $Q \simeq 0$), and the α particles would have a broad distribution around 4/5 of the energy of ^{5}He (Fig. 3c).

In addition, the relatively large energy of the observed α particles, which increases with the projectile energy, suggests a direct process rather than a compound nucleus mechanism.

Both the DBU and TC calculations make use of the di-neutron model discussed above. The NT calculations were done in DWBA, and included the bound states of the ^{209}Pb nucleus. The details of these three calculations, such as the interactions parameters,

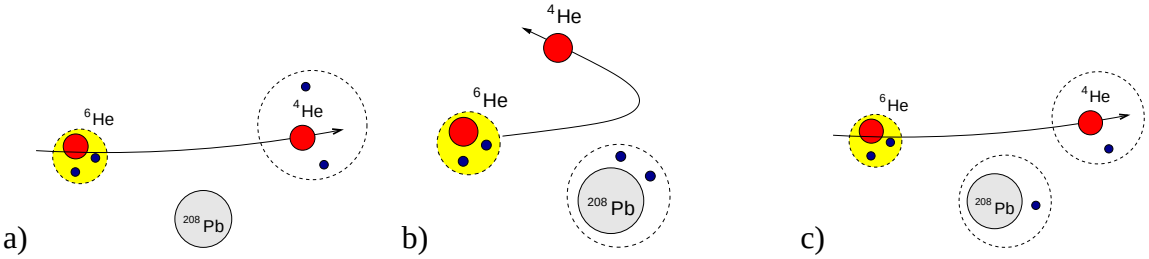

FIGURE 3. Three different reaction models for the production of α particles in the ^{6}He+^{208}Pb reaction: a) direct breakup, b) transfer to the continuum and c) one-neutron transfer.

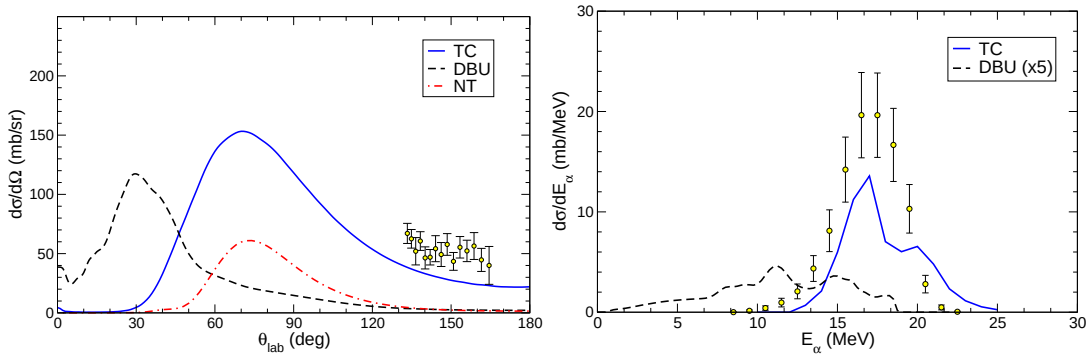

FIGURE 4. Left: Angular distribution of the α particles arising from ^{6}He fragmentation, in the laboratory frame, for $E_{\rm lab}$=22 MeV. The experimental distributions are compared with transfer to the continuum (TC) calculations (solid lines), CDCC (DBU) calculation (dashed line), and a DWBA calculation for the one neutron transfer (NT) leading to bound states of the ^{209}Pb nucleus (dotted-dashed line). Right: Angle-integrated energy distributions of α particles. The direct breakup component has been multiplied by a factor of 5.

are given in Ref. [17]. The results of the calculations are presented in Fig. 4. The left panel shows the angular distribution of the measured α particles, whereas the right panel corresponds to the energy distribution, integrated in the scattering angle ($\theta_{\rm lab} = 132^\circ - 168^\circ$). The solid lines in both panels correspond to the TC calculation. This calculation accounts very well for the shape of the energy distributions and is also in fair agreement with the absolute magnitude of the data. By contrast, the DBU (dashed line) and NT calculations (dotted-dashed line) predict too small cross section in the angular region of interest. Moreover, the DBU calculation underpredicts the energy of the α particles.

Thus, these results suggest a scenario in which the valence neutrons of the ^{6}He projectile are captured by the target, and the remaining α particle is accelerated with respect to the beam velocity. These picture is consistent with previous experimental results for other reactions induced by ^{6}He, in which large transfer cross sections have been observed [3, 4].

SUMMARY

We have presented and discussed recent experimental data for the reaction ^{6}He+^{208}Pb at energies around the Coulomb barrier. The elastic scattering angular distribution shows a significant suppression with respect to the Fresnel behaviour observed in tightly bound projectiles. An OM analysis shows that these data can only be reproduced using optical potentials with large values for the diffuseness of the imaginary part. This suggests the presence of long range absorption mechanisms. Three-body (di-neutron) and four-body CDCC calculations accounted very well for the data, and confirm that these long range mechanisms are mostly related to the strong couplings to the continuum states. Finally, the angular and energy distributions of the prominent group of α particles observed at backward angles have been analyzed using different reaction models. These distributions could be well reproduced assuming a transfer to the continuum mechanism, in which the neutrons of the halo are transferred to very excited states of the target, in the proximity of the two-neutron breakup threshold. However, the calculations assuming a direct breakup or a one-neutron transfer mechanism failed to describe the data.

ACKNOWLEDGMENTS

This work has been partially supported by the Junta de Andalucía, under project P07-FQM-02894, by the Spanish Ministerio de Educación y Ciencia under projects FIS2008-04189, FPA2006-13807-c02-01, FPA2007-62170, FPA2007-63074 and by the Spanish Consolider-Ingenio 2010 Programme CPAN (CSD2007-00042). A.M.M. acknowledges a research grant by the Junta de Andalucía.

REFERENCES

1. O. R. Kakuee, et al., *Nucl. Phys.* **A728**, 339 (2003).
2. O. R. Kakuee, et al., *Nucl. Phys.* **A765**, 294 (2006).
3. A. Di Pietro, et al., *Phys. Rev. C* **69**, 044613 (2004).
4. E. F. Aguilera, et al., *Phys. Rev. Lett.* **84**, 5058–5061 (2000).
5. A. R. Barnett, and J. S. Lilley, *Phys. Rev. C* **9**, 2010 (1974).
6. A. M. Sánchez-Benítez, et al., *Nucl. Phys.* **A803**, 30 (2008).
7. N. Keeley, J. M. Cook, K. W. Kemper, B. T. Roeder, W. D. Weintraub, F. Marechal, and K. Rusek, *Phys. Rev. C* **68**, 054601 (2003).
8. A. M. Moro, K. Rusek, J. M. Arias, J. Gómez-Camacho, and M. Rodríguez-Gallardo, *Phys. Rev. C* **75**, 064607 (2007).
9. W. W. Daehnick, J. D. Childs, and Z. Vrcelj, *Phys. Rev. C* **21**, 2253 (1980).
10. K. Rusek, I. Martel, J. Gómez-Camacho, A. M. Moro, and R. Raabe, *Phys. Rev. C* **72**, 037603 (2005).
11. T. Matsumoto, E. Hiyama, K. Ogata, Y. Iseri, M. Kamimura, S. Chiba, and M. Yahiro, *Phys. Rev. C* **70**, 061601 (2004).
12. T. Matsumoto, T. Egami, K. Ogata, Y. Iseri, M. Kamimura, and M. Yahiro, *Phys. Rev. C* **73**, 051602 (2006).
13. M. Rodríguez-Gallardo, J. Arias, J. Gómez-Camacho, R. Johnson, A. Moro, I. Thompson, and J. Tostevin, *Phys. Rev. C* **78**, 064609 (2008).
14. M. Rodríguez-Gallardo, J. M. Arias, J. Gómez-Camacho, A. M. Moro, I. J. Thompson, and J. A. Tostevin, *Phys. Rev. C* **72**, 024007 (2005).

15. A. M. Moro, J. M. Arias, J. Gómez-Camacho, I. Martel, F. Pérez-Bernal, R. Crespo, and F. Nunes, *Phys. Rev. C* **65**, 011602 (2002).
16. M. Rodríguez-Gallardo, et al., *Submitted for publication* (2009).
17. D. Escrig, et al., *Nucl.Phys.* **A792**, 2 (2007).